Calibration Techniques for Digital Phased Arrays

C. Fulton, W. Chappell

Purdue University, West Lafayette, Indiana, 47907, USA

***Abstract* — Several techniques for calibrating and aligning different aspects of a digital phased array are demonstrated using a 16-element, panelized, vertically-polarized S-band subarray with element-level digitization on both transmit and receive. These techniques make use of the element-level functionality not only to expedite the process of initial alignment and calibration but to enhance the ability of the array to maintain and enforce this calibration over time as RF/analog system variations occur. A method for maintaining element amplitude and phase over time in fully digitized arrays is demonstrated as well as a technique for element-level self-calibration of quadrature mismatches.**

***Index Terms* — Calibration, phased array radar**

I. Introduction

Active phased array systems require some level of calibration in order to perform optimally. While the details and extent of this calibration vary from system to system, virtually all of them require that each element's amplitude, phase (or time delay), and even polarization are set correctly to achieve the desired beam pattern. There are various techniques to determine what these effective weights should be, given that each element in a finite array will have a slightly different pattern and/or frequency variation caused by mutual coupling and scattering due to the finite nature of the array. These patterns, as well as the active circuitry, must be simulated or measured as part of an initial calibration procedure requiring equipment external to the phased array. Past examples of this type of calibration include [1-3]; in each of these works, the goal was to utilize pattern information from each individual antenna to synthesize good overall patterns. This is necessary in order to precisely control the sidelobe levels and the depth and location of any nulls, all of which are critical in any phased array, especially one with the potential to perform adaptive beamforming to suppress jammers or interference. Throughout this paper, this type of calibration—which concerns how the passive antenna array radiates—will be called "external calibration."

The other type of calibration, "internal calibration," deals with the variations over time and from element to element in how the antenna panel interacts with the active circuitry and control system itself. This may include, for example, quadrature (I/Q) balancing, adaptive channel equalization, and gain/phase compensation of active components over a wide range of power levels and temperatures. Usually, both the internal and external calibrations are initially performed in an anechoic chamber with external equipment, but it is often necessary to update the internal calibrations once the array has been fielded, since analog components inevitably change their characteristics as they age and respond to their environment, and they might even need to be replaced. There are therefore two important differences between internal and external calibration that warrant the distinction between them. Nominally, a fielded radar effectively looks out into free space, and the physical antennas themselves do not change over time nearly as much as the analog/active circuitry will; thus, updates to the external calibration are expected to be made much less often than internal calibration updates. The other important difference is that an update to the external calibration usually requires equipment in the far field of the antenna and/or an anechoic chamber, whereas updates to the internal calibration may not.

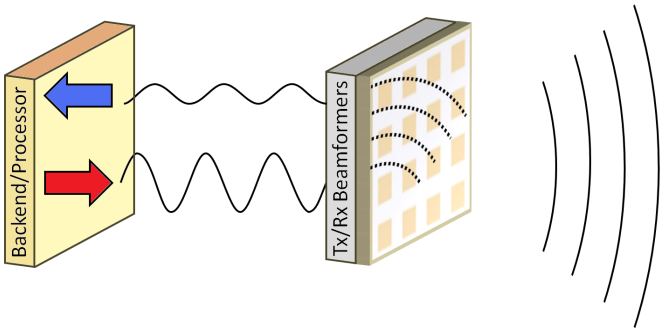

Figure 1: Illustration of mutual coupling-based calibration monitoring using internal array hardware only.

In fact, past work has demonstrated that internal calibration of finite arrays can be updated and maintained by measuring the coupling from each antenna element to some sort of calibration device located near or in the array itself [4], [5] or even the coupling between different antenna elements [6], [7] as shown in Fig. 1. The initial coupling values or waveforms are recorded during the initial array alignment in an anechoic chamber. After the system is fielded, these coupling measurements are monitored to determine and possibly even correct any changes to the performance of each element. However, many traditional systems cannot transmit arbitrary waveforms on one or more elements and simultaneously receive on others in order to make these measurements; others only have access to the output of the analog beamformers and not the individual elements. Systems like the ones used in [4], [5] require additional analog circuitry for the dedicated internal calibration equipment. Additionally, the techniques used in [6], [7] require that mutual coupling symmetry arguments apply throughout the array, which is only valid for certain element types in a large enough array.

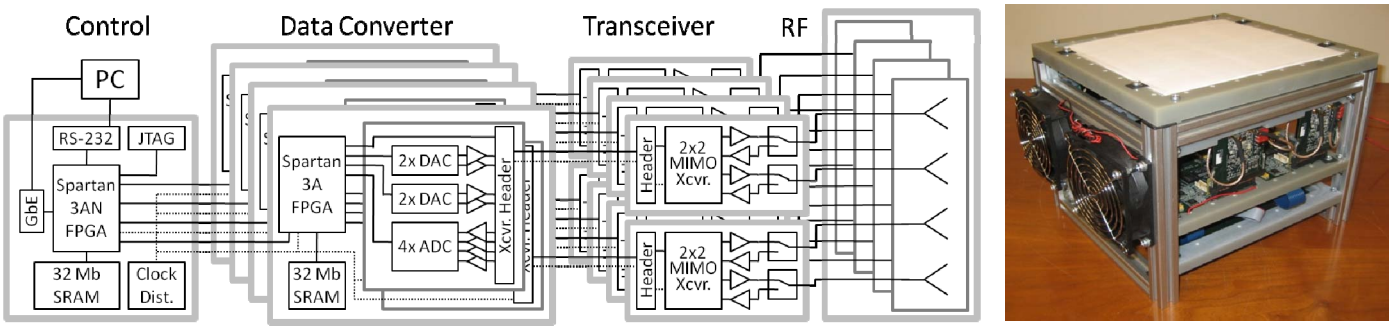

Figure 2: System block diagram and photograph of DAR prototype

Of course, analog beamformers can have inherent limits on beamforming itself. Those with a few bits of phase or amplitude control have limited beam quality and bandwidth, and multiple beamformers are needed for multiple beams. As demands on radar functionality and performance continue to increase, so does the need for flexible and adaptive phased arrays with multi-beam capability. With these demands has come a trend of increased digitization of signals, and the analog-to-digital conversion point is moving closer to the elements themselves. The amount of data that must be handled and processed is increasing accordingly, but digital systems promise to advance and scale to accommodate this. Eventually, it will be both desirable and practical to digitize signals at the element level. With such a system, it may be possible to overcome some of the aforementioned limitations to calibration (and, in general, beamforming) by leveraging new tools afforded by the ability to independently and simultaneously generate and analyze waveforms on each of the elements with precise amplitude, frequency, and phase control.

The Digital Array Radar (DAR) subarray is a prototype of this type of phased array, where each element's signals are digitized separately on both transmit and receive. A modified version of the mutual coupling-based techniques described above is implemented on this system to show that the internal calibration of the array can be maintained. In particular, we demonstrate how mutual coupling values measured during the initial calibration procedure can be used to monitor the amplitude and phase of each element and that detected errors can subsequently be corrected. A technique is also presented for automatically balancing the in-phase (I) and quadrature (Q) channels on each of the direct conversion transceivers used in the DAR system. A brief introduction to the relevant features and operation of the DAR system is presented in Section II before these calibration are detailed in Sections III and IV.

II. DAR System Details

A system block diagram and photograph of the DAR system adapted from [8] is shown in Fig. 2. The prototype consists of a set of eight commercial-grade, 2-channel, direct conversion transceiver ICs to drive a 4x4, linearly polarized stacked patch antenna array at S-band (3.1-3.5 GHz) [9]. The transceivers connect to digital panels, which have 12 bit, 24 MSPS ADCs and DACs for the quadrature (I and Q) signals for each element's transmit and receive signals. The sampling clock is coherent among all elements and is distributed hierarchically through the digital backend. The transceivers themselves, which have a maximum bandwidth of 7 MHz (or a complex baseband bandwidth of 14 MHz), are digitally programmable to have different gains, filter bandwidths, baseband DC offsets, and more. Each transceiver chip also has an on-chip fractional-N PLL which is shared between its pair of transceivers. A reference signal at 40 MHz is distributed to each transceiver, from which the RF local oscillators (LO) are derived and phase locked. This clock is also divided down to 10 MHz and buffered so that it can be used to phase-lock RF test equipment during initial alignment.

The received digital streams are fed to a flexible hierarchical digital beamformer with low-level processing so that the data can be post-processed. Element weighting and quadrature imbalance correction are performed digitally at each element, as described in Section IV. The system supports two modes of operation: one where a single real-time receive beam from the digital beamformer is sent through the Gigabit Ethernet connection and another where data that is simultaneously collected from each receiver and stored in RAM can be streamed to the host PC whenever it is required. The system has direct digital synthesizers (DDSs) for each element's transmitter. These synthesizers can be programmed to generate constant tones or pulsed LFM (linear frequency modulated) complex baseband tones with complex weights. Additionally, each DDS can apply small amplitude, phase, and DC offset differences between the I and Q channels for quadrature balancing. The entire digital system is implemented on a set of low-cost FPGAs that interface to a host PC that runs a full-featured graphical user interface with control of element-level settings, beam steering, post-processing, and system configuration.

III. Element Alignment

Regardless of whether the beamforming is performed digitally or in the traditional analog fashion, the chief concern in active phased array calibration is to establish the correct amplitude and phase for each of the elements in order to control the radiation patter. After a general discussion on the issues

involved in initial internal and external calibration, this section details how mutual coupling "measurements" performed on and by the DAR system itself are used to record and subsequently enforce the initial internal and external calibrations.

A. Initial Element Alignment

The introduction outlined some of the past work in the area of initial array calibration. The theoretical aspects of initial array calibration are well-covered in the literature, but there are practical concerns that must be addressed as well. An excellent overview of the analysis and modeling of practical phased array radiation characteristics is given by Kelley and Stutzman [1]. In it, an exact analysis of a general array reveals that the overall field pattern of the array can be written as (using [a]'s notation):

$$E(\theta,\phi) = \sum_{q=1}^{N_s} V_q g_n^q(\theta,\phi), \qquad (1)$$

where N_s is the number of elements, V_q is the voltage at the generator of the qth element (with a common source impedance of Z_q at all elements), and $g_n^q(\theta,\Phi)$ is the *unit-excitation active element pattern* that needs to be determined. Lumped into this pattern are all the effects caused by variation in element pattern due to their physical location away from the phase center of the array, variations in the elements themselves, variations in active circuitry among elements, finite array effects, and the effect of the active (driving-point) input impedance of each element. In order to take these effects into account, each element must be measured over a range of angles while the array is in operation. The patterns are then fit to a model that is an abstraction of (1) to a form more amenable for pattern synthesis, such as the classic product of an array factor and an element factor [3]. The work in [2] applies this technique to a receive-only array that is similar to the DAR prototype. This process typically requires more than just amplitude and phase alignment at broadside, and the number of measurements that need to be made for the initial calibration can be very large.

Among the important practical considerations in these measurements is whether or not it is feasible to measure both amplitude and phase of the radiated or received fields. There are methods for fast calibration when phase can be measured, even if individual elements cannot be turned on and off separately [10]. Nominally, one would be able to perform network analyzer-like measurements between the phased array elements and the far-field, but in many systems this is not possible. In this case, multiple power measurements can be made to extract the phase [11], [12]. Fortunately, the DAR system can be phase-locked to an external signal generator, as indicated in Section II. Since digitization is performed at the element level simultaneously, the amplitudes and phases of each receive element can be readily calculated for an incoming plane wave in a given direction. The signal generator's frequency is set to the RF LO frequency of the transceivers so that the measured amplitude and phase of the DC values of the I/Q channels reflect the complex antenna weight. If the DC offset present in these channels can be kept below -40 dB relative to the strength of the signal itself, the error of the measured complex weight will be less than 1%. This corresponds to a maximum amplitude error of 0.09 dB or phase error of 0.6º, which should be sufficient. The next section details how this DC offset can be suppressed even further than that. Even if the plane wave source is not phase-locked to the receiver, the measured relative phases between the elements will still be valid. An element-level digital receive beamformer thus expedites some of the difficult measurements commonly made for external calibration of analog beamformers, especially when thousands of measurements need to be made to fit to a model like (1).

For the purposes of demonstrating the process described above, the DAR system's receivers were aligned at broadside, and the resulting weights were also stored for use in the next subsection. For broadside alignment, the product of each V_q and its associated unit excitation active element pattern at broadside is set to a constant. The resulting receive difference patterns are shown in Fig. 3, where linear phase shifts across the array are applied to scan the null. The null depth and sidelobe levels are good until the array is scanned beyond 30º, where the unit excitation active element patterns of the elements begin to differ from one another by more than just a phase shift due to spatial displacement from the antenna center. The model in (1) could be fit at more angles than broadside to improve this if desired, as in [2].

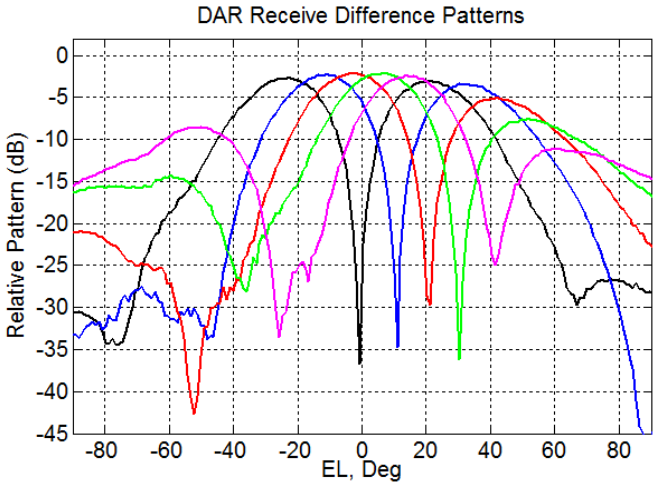

Fig. 3. Measured receive difference patterns for DAR prototype, showing effects of finite array at higher scan angles

In the DAR system, the alignment of the transmitters is not as trivial as that of the receivers because complex transmissions from multiple antennas cannot be easily measured simultaneously. However, amplitude and phase can still be measured for each antenna individually. This is accomplished in the DAR system by transmitting a constant tone from the signal generator at the RF LO frequency, spatially combining it

with each transmitter sequentially, and measuring the subsequent received power level. The phase of each transmitter is rotated from its default value in order to extract the relative amplitude and phase, similar to the power-based measurement method described in [11]. After aligning at broadside, as with the receivers, the measured transmit sum patterns are as shown in Fig. 4, where linear phase shifts are again applied to steer the beam. They are compared to simulated patterns of the 4x4 patch array by itself without the effects of the aluminum frame and mounting hardware.

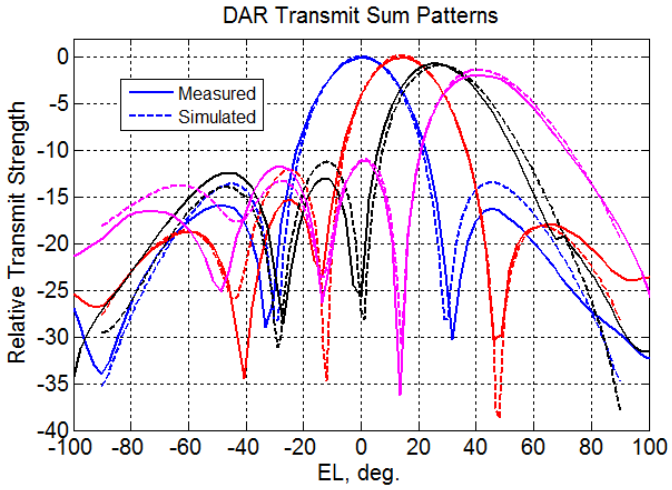

Fig. 4. Measured transmit sum patterns for the DAR prototype after external calibration compared to a free-space simulation. Beam scanned at 0º, 15º, 30º, and 45º.

The patterns achieved with only one measurement at broadside may be sufficient in some cases. For very large arrays, the argument can be made that most of the elements—especially elements near the center of the array—will have the same characteristics in active impedance and pattern because of periodicity in the (nearly infinite) array. Under these conditions, the overall pattern (1) can be rewritten as [a]:

$$E(\theta,\phi) = g_{av}(\theta,\phi)\sum_{q=1}^{N_s} V_q e^{jk\mathbf{r}\cdot\mathbf{r_q}} \quad , \qquad (2)$$

where now $\mathbf{r_q}$ is the qth element's location and the pattern $g_{av}(\theta,\Phi)$, called the *average active element pattern,* is factored out since it varies little throughout the array. All calibration then needs to do is equalize the amplitudes and phases of the active circuitry to be able to enforce known V_q values.

In fact, in both [6] and [7], these semi-infinite array ideas are extended even further to argue that the mutual coupling between adjacent elements must not vary from element to element either. By "measuring" this mutual coupling between one element and pairs of other elements for which symmetry arguments apply, the differences between the receivers of these elements can be canceled out. The transmitters are calibrated in this way as well. The procedure is then cascaded throughout the array. This is a very attractive calibration routine, as both the external and internal calibration can be done without external equipment. There other problems with these calibration techniques, though. As implemented in [6] and [7], the mutual coupling measurements are made between adjacent elements. In an active array with a transmit power that is more than a few Watts per element, this may easily saturate any practical receiver, given that coupling between adjacent elements can be on the order of as much as -10 dB. Additionally, as pointed out by [4], these techniques may be prone to errors caused by coupling and finite isolation between the analog transmit and receive beamformers that complicate the ability to truly turn on only one transmit element and listen to only one receive element at a time. In a digital phased array like the DAR prototype, however, these beamformers are completely digital, and thus the worrisome coupling is exactly zero. The DAR system would also allow for multiple simultaneous coupling measurements to be made (see Fig. 1), as it can analyze the receiver outputs individually to determine which, if any, are being saturated, and only use information from receivers that are not being saturated. A large digital phased array with a similar architecture to that of the DAR prototype would thus be a good candidate for a similar calibration procedure. This is the subject of the following subsection.

B. Monitoring and Correcting Internal Calibration Errors

Once the initial internal and external calibration is complete and all elements are aligned for the scan angles and frequencies of interest, it is important to be able to monitor the quality of this calibration once the array has been fielded. As discussed in the introduction to the paper, this internal calibration monitoring is a distinctly different challenge than the initial calibration. The purpose is to ensure that aspects of the system that may change with time—for example, gain and phase drift in power amplifiers, and even failures of active elements—can be effectively monitored and compensated. If the assumption can be made that the passive antennas themselves are not modified or damaged and that their radiating characteristics do not change with time, then it should be possible to perform this internal calibration without returning the array to an anechoic chamber or bringing expensive far-field test equipment out to re-calibrate the array.

The same practical issues that limit the applicability of the adjacent element coupling techniques in used in ([6], [7]) may cause similar problems in traditional analog active arrays. Many systems thus make use of internal calibration devices for this function as illustrated before in Fig. 1. The performance-monitoring and fault correction system in [5], for example, embeds a microstrip line into the antenna panel that couples with each element in the array in order to sense changes from an initial measured coupling made in the far-field chamber in which the external calibration is performed. This requires additional hardware and an initial calibration of the calibration equipment itself, and it may not be possible to

detect and correct for changes in the calibration hardware. The idea of mutual coupling-based internal calibration is taken a step further in [4], where actual elements are dedicated solely to calibration. The number of such elements must be limited, though, to keep from interfering with radar operation. This forces the calibration elements to be spaced far apart, which places constraints on the dynamic range and overall number of mutual coupling measurements that can be made for a given element.

Nevertheless, these techniques have proven to be effective at maintaining system performance over long periods of time. As mentioned in the first part of this section in the context of using mutual coupling for performing the initial alignment, the DAR system does not have problems caused by finite isolation between transmit and receive beamformers while mutual coupling measurements are made. Additionally, when the DAR system transmits from any given element, it can utilize coupling values to all receiver elements whose signal level is in an optimal region of the receiver's dynamic range; this provides an averaging effect to the coupling measurements.

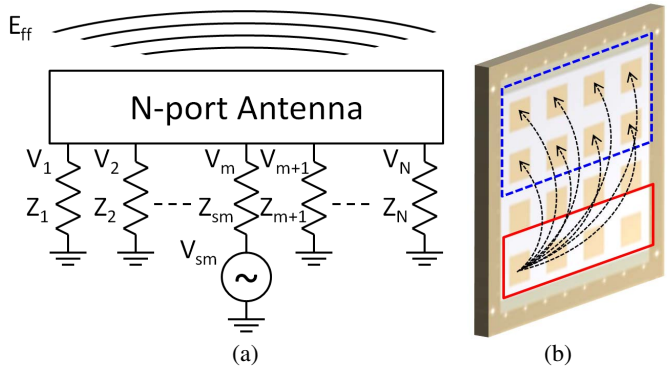

Fig. 5. DAR system mutual coupling: (a) coupling model and (b) coupling scheme used in this demonstration.

In the DAR system, the mutual coupling in the antenna panel between elements can be modeled with an N-port that is excited by a Thévenin equivalent source at the transmit port while the other N-1 ports are terminated in their effective impedances, as shown in Fig. 5. If these impedances can be assumed to be constant with time, then V_m and E_{ff} will always have the same relationship as they did in the initial calibration unless the antenna is damaged or interfering objects are present in the near-field. Denote the ratio of the digitized complex amplitude and phase at the n^{th} receiver when the m^{th} transmitter is excited at its nominal digital amplitude and phase as C_{mn}. This is the mutual coupling value that is recorded right after the initial calibration. Denote any subsequent multiplicative change in the ratio between the V_ns at the receivers and the digitized amplitude and phase by R_n and, similarly, the subsequent multiplicative change in the ratio of the digital transmit amplitude and phase to the transmit voltage V_m as T_m. Under the assumptions above, subsequent mutual coupling measurements made after changes occur in the analog components will then have a value of

$$C'_{mn} = T_m R_n C_{mn} . \tag{3}$$

Dividing this by the original coupling value, we obtain the following coupling metric matrix:

$$K_{mn} = \frac{C'_{mn}}{C_{mn}} = T_m R_n \tag{4}$$

This coupling matrix can then be used to estimate the deviations in the transmitters and receivers used in the measurement.

Consider a coupling scheme for the 4x4 DAR array, where the bottom four elements transmit and the top eight receive, as shown in Fig. 5b with the first transmitter turned on. The coupling values for this set of transmit and receive elements happen to be such that the received signal levels are in the optimal range for the bi-static tracking demonstration described in [8]. This procedure could be performed on other groups of elements in the array to align all receivers and transmitters. For a system like this with individual control of the elements, one is able to choose from a vast array of coupling values from any given transmitter in order to select which receivers to use in which transmitting group. For the couplings in Fig. 5b, the ideal K matrix is explicitly written as:

$$\mathbf{K} = \begin{bmatrix} T_1R_1 & T_1R_2 & T_1R_3 & T_1R_4 & T_1R_5 & T_1R_6 & T_1R_7 & T_1R_8 \\ T_2R_1 & T_2R_2 & T_2R_3 & T_2R_4 & T_2R_5 & T_2R_6 & T_2R_7 & T_2R_8 \\ T_3R_1 & T_3R_2 & T_3R_3 & T_3R_4 & T_3R_5 & T_3R_6 & T_3R_7 & T_3R_8 \\ T_4R_4 & T_4R_2 & T_4R_3 & T_4R_4 & T_4R_5 & T_4R_6 & T_4R_7 & T_4R_8 \end{bmatrix} . \tag{5}$$

It is important to note that if all transmitters change by a complex value X and all receivers change by a complex value $1/X$, then the coupling matrix **K** will have a value of 1 for all entries. Thus, there exists an arbitrary *reference value* for all transmitters and receivers that must be chosen wisely based on the system's known characteristics. For the DAR system, like many arrays, one may presume that the receivers suffer from amplitude changes that are less severe than those of the transmitter, which may have a high power amplifier whose output power changes significantly with temperature. Under this assumption, one may estimate the amplitude of the m^{th} transmitter relative to the others as:

$$|T_m| = \sum_n |K_{mn}| . \tag{6}$$

Values measured in (5) may have small errors due to noise, small nonlinearities, and slight changes to the impedances Z_n of the receivers, but the summation in (6) provides an averaging effect for estimating the T_m values. The amplitude and phase of the transmitter with the median power is then selected as the arbitrary reference value on which corrections will be made. This is merely one option of many. At this

point, it should be clear if any transmitters have failed and need to be replaced. The next step is to align the transmitters to each other. This is done by dividing each row of (5) by the row corresponding to the reference transmitter, forming a matrix **K'** whose elements are, in the absence of errors, equal to $K'_{mn} = T_m/T_p$, where p is equal to the index of the reference transmitter. Averaging along the rows of K' then gives the estimated values of T_m. Once the values of the T_m are estimated, the mth row of **K** is divided by T_m, and the R_n values are obtained from the average along the columns of the resulting matrix. Digital weights of $1/T_m$ and $1/R_n$ are then applied to the m^{th} transmitter and the n^{th} receiver, respectively, to correct for the detected drift in their amplitude and phase.

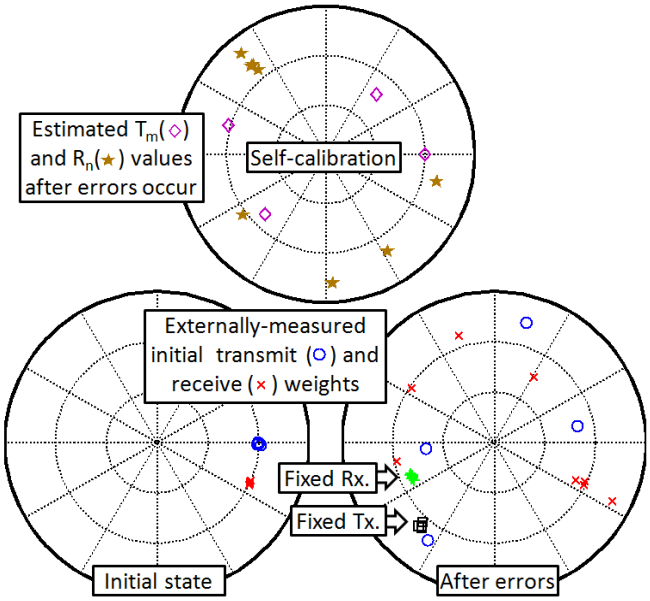

Fig. 6. Correction of randomly-induced errors using mutual coupling technique: (left) externally-measured initial state, (top) calibration-detected errors, and (right) externally-measured errors before and after correction

To demonstrate this procedure in operation on the DAR system, the transmitters and receivers were initially aligned to each other in the chamber, as shown on the normalized complex weight plot on the left of Fig. 6, and the initial mutual coupling measurements were recorded. Note that there is a phase shift between the transmitters and receivers that must remain fixed with respect to each other, but not to the external measurement equipment. To simulate an extreme version of gain and phase drift, random amplitude and phase errors were then introduced by modifying gain settings on the transceivers and applying offsets to digital phase shifters, as shown in the right complex weight plot. The internal calibration procedure was then run, and the resulting T_m and R_n values are shown on the top complex plane plot. After applying the digital corrections, the resulting externally-measured transmit and receive weights are as shown superimposed on the right. Not only are the transmitters re-aligned to each other (and the receivers to each other), but the phase between the transmitter and receiver stays unchanged; this may be a requirement in some applications. Note that the phase of the aligned transmitters and receivers relative to the external equipment has changed, but this should not matter. There is also a measured amplitude difference between the normalized transmitters and the normalized receivers, and this is because the transmitter that was used to set the reference gain and phase happened to have a slightly higher than nominal gain value. This is a consequence of having to pick a reference value during the procedure.

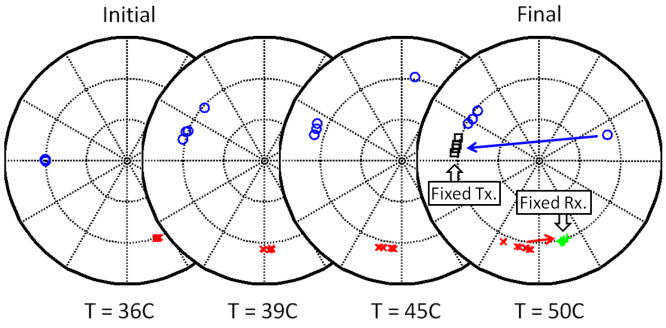

Fig. 6. Correction of errors due to local heating on array.

As a test of this procedure in a more realistic scenario, a heat gun was pointed at one corner of the array to simulate local heating on one of the transmitters as well as an overall temperature change throughout the array. The results of this test are shown in Fig. 6, where all points of data were measured with the external equipment as before and the temperatures were measured on the corner transmitter's power amplifier IC. As the transmitter on the corner of the array heated up, its phase began to drift significantly—to the point of destructively interfering with the other transmitters. As the other transmitters and receivers heated up, they also began to slightly drift in phase. After the application of the self-calibration procedure to fix the internal alignment, the transmitters were aligned to within ±7°, and the receivers were aligned to with ±2.5°. The amplitudes of the receivers were restored, and the phase between transmitters and receivers was recovered to within a few degrees. The small residual errors are likely due to changes in impedance seen by the antenna panel—the Z_n in figure 5a—which were assumed to be invariant with time, or they could be caused by heating of the antenna array itself. These second-order effects may need to be considered in some applications.

III. Quadrature Balancing of Transceivers

A. Introduction and Description of Problem

In addition to internal calibration to preserve element alignment, the mutual coupling technique can be used to characterize other non-idealities in the signal chain behind the antennas themselves. This section details an example of this kind of correction wherein automatic gain, phase, and DC offset correction is performed on the I and Q channels of each transceiver. The direct conversion transceiver ICs used in the DAR subarray require no external image filters, have two full transceivers per chip, and provide register-level access to gain, bandwidth, and frequency synthesizer controls over a simple

digital interface. In this respect, they represent a step towards the highly-integrated, low-cost RF transceiver solutions that promise to deliver future phased arrays with less than one IC per element. While the low intermediate frequency also offers the chance to oversample the baseband signals more easily, the architecture itself suffers from imbalances in the in-phase and quadrature (I/Q) channels since the final down-conversion to complex baseband is done directly with analog components. The analog components in the system, including the quadrature mixers and all baseband analog buffers and data converters, will affect the I and Q signals differently, causing them to be deviate from being 90º out of phase and to have different amplitudes. This causes "image" spurs to appear on the opposite side of the complex baseband spectrum. Additionally, on transmit, any leakage of the RF LO or DC offsets on the I or Q signals leads to an undesired tone at that frequency, and self-mixing of the LO on receive leads to DC offsets in the digitized outputs, as do any offsets in baseband buffers or filters.

These effects degrade the performance of both communication and radar systems and should be minimized as much as possible as part of the internal calibration procedure. The image frequency component is particularly a problem in radar systems that use a pulse Doppler processor, where the system will show a false target at the image Doppler frequency [13], the relative return of which having the same ratio to the main target return as that of the image spur to the main tone in the pulse waveforms. For example, an image spur in the transmitter that is 20 dB below the main tone would cause a false target to appear only 20 dB below the main target, which could easily lead to false alarms. Additionally, there is a problem with using chirped LFM waveforms because the image frequency component causes what is, in effect, an additional DC component in the output to the matched filter; this causes the time domain output sidelobes to rise, limiting target detection. However, this effect lessens with larger bandwidth-pulse width products [14]. The effect on communication systems is, for example, to stretch and skew the constellation of a quadrature-modulated signal. Finally, the presence of DC offsets in the receivers and LO feed-through on transmit may limit the ability to perform the external calibrations described in Section III.

B. Modeling and Calibrating DAR Quadrature Imbalance

A model for quadrature imbalance over a narrow frequency range in a general direct conversion transmitter is presented in Fig. 7. Though the sources of the imbalances and offsets may be different in the receive case, the effective model for the imbalance is exactly the same as in the transmit case, but the signal paths are reversed. Define the gain and phase imbalances as ΔG and $\Delta\Phi$, respectively, and the DC offsets as I_{DC} and Q_{DC}. The signals sent to the DACs by the digital backend are the discrete versions of $x_I(t)$ and $x_Q(t)$, which are then filtered by analog circuitry to form their continuous-time counterparts. At the baseband frequency, ω_B, the gain blocks represent the difference in gain between the I and Q channels due to filtering, amplifier imbalance, the DACs themselves, and even the mixers. The phase imbalance $\Delta\Phi$ represents phase difference between these two analog channels as well as the deviation from 90º between the inputs to the mixers. The local oscillator $y_{LO}(t)$ is nominally a pure tone at the center of the RF transmit band (ω_{LO}), and the output signal is $x_{RF}(t)$.

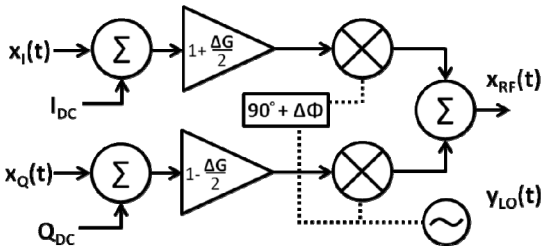

Fig. 7: I/Q imbalance model block diagram

If one were to send to transmit the signals $x_I(t) = \cos(\omega_B t)$ and $x_Q(t) = -\sin(\omega_B t)$ to generate an RF tone at $\omega_{LO}+\omega_B$, the output could be written as be

$$x_{RF}(t)=\left(1+\frac{\Delta G}{2}\right)\cos\left(\omega_{LO}t+\theta_0+\frac{\Delta\Phi}{2}\right)\left[\cos(\omega_B t)+I_{DC}\right] + \left(1-\frac{\Delta G}{2}\right)\sin\left(\omega_{LO}t+\theta_0-\frac{\Delta\Phi}{2}\right)\left[-\sin(\omega_B t)+Q_{DC}\right], \quad (7)$$

which, after several trigonometric expansions can be approximated by

$$x_{RF}(t)\approx\cos\left(\left[\omega_{LO}+\omega_B\right]t+\theta_0\right)+x_{IM}(t)+x_{LO}(t), \quad (8)$$

where

$$x_{IM}(t)=\frac{\Delta G}{2}\cos\left(\left[\omega_{LO}-\omega_B\right]t+\theta_0\right)-\frac{\Delta\Phi}{2}\sin\left(\left[\omega_{LO}-\omega_B\right]t+\theta_0\right) \quad (8a)$$

$$x_{LO}(t)=I_{DC}\cos(\omega_{LO}t+\theta_0)+Q_{DC}\sin(\omega_{LO}t+\theta_0), \quad (8b)$$

by assuming that ΔG, $\Delta\Phi$, I_{DC} and Q_{DC} are small enough to use first-order approximations (e.g. $\sin(\Delta\Phi)\approx\Delta\Phi$). The first term in (8) is the desired tone at $\omega_{LO}+\omega_B$, the term in (8a) is the image tone at $\omega_{LO}-\omega_B$ caused by gain and phase mismatch, and the term in (8b) is caused by DC offsets (or, equivalently, LO leakage through the output of the transmitter). It is important to note that not only are these frequencies exact (despite the approximations), but they are the only frequencies that are generated by this linear model. However, non-linearities in the mixing stage and subsequent power amplifiers can cause these tones to mix with each other or with the LO to generate other tones at integer multiples of the baseband frequency away from the LO ($\omega_{LO}+n*\omega_B$).

In order to compensate for quadrature imbalance, the parameters ΔG and $\Delta\Phi$ as well as the DC offsets and/or LO feedthrough must be directly or indirectly estimated. For communications applications, techniques have been developed to

calibrate receivers using quadrature modulated RF waveforms of a known type, examining the acquired baseband samples, and forming estimates of the values of ΔG and $\Delta\Phi$ [15]. However, if one had access to a monochromatic (CW) source at the input to a direct-conversion receiver tuned at a slightly different frequency, calculation of the exact quadrature imbalance parameters would simply require analysis of the received waveform. Similarly, on transmit, if one had access to a spectrum analyzer and could transmit a constant baseband tone and examine the relative levels of the three tones in (8), it would be possible to calibrate the transmitter. This is precisely the approach used in [16], where a complex iterative algorithm is used for this internal transmit calibration. As demonstrated in the previous section, the DAR system has the ability to transmit from one element, receive on another through mutual coupling, and perform spectral analysis, so it should be able to perform this calibration without external equipment. However, if the transmitting element and the receiving element share the same RF LO, it would be impossible to separate the quadrature imbalances due to the transmitter from those of the receiver; for example, if the transmitter generates a baseband tone at 1 MHz with an LO of 3.3 GHz, it will generate a main tone at 3.301 GHz, LO leakage at 3.3 GHz, and an image tone at 3.299 GHz. The receiver would see the 3.301 GHz and 3.299 GHz tones and generate its own additional image tones from these. The 3.3 GHz LO will simply add to the DC offset that was already present on the receiver.

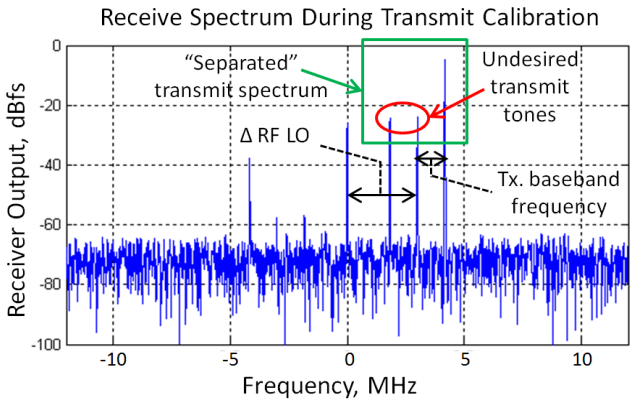

Fig. 8. Illustration of separation of transmit and receive tones due to quadrature imbalance. The middle transmit tone is due to DC offsets at baseband and LO feed-through, and the transmit tone on the left is due to gain and phase mismatch between I and Q channels.

The solution to this problem is to have the receiver tuned to a slightly different LO, which has the effect of separating the imbalance tones due to the transmitter from those of the receiver. The DAR system has independent control over the eight transceiver frequency synthesizers, so this is possible as long as the transmitter and receiver do not share the same IC. Specifically, consider a transmitter whose LO is set to ω_{TX} with a baseband frequency of ω_B and a receiver whose LO is set to ω_{RX}. The main transmit tone at $\omega_{TX} + \omega_B$, the tone due to LO leakage at ω_{TX}, and the image tone at $\omega_{TX} - \omega_B$ will appear in the receiver's output as three separate "main tones" at $\omega_{TX} - \omega_{RX} + \omega_B$, $\omega_{TX} - \omega_{RX}$, and $\omega_{TX} - \omega_{RX} - \omega_B$. These three tones will also cause their own image tones at the receiver, and there will be a DC offset (due to the receiver alone). An example of this is illustrated in Fig. 8. The three main tones due to the transmitter will, assuming negligible receiver filtering effects, reflect the same relationship between their power levels as they would on an RF spectrum analyzer.

An iterative procedure is then used to eliminate the transmitter's quadrature imbalance. From (8), the power levels of the undesired tones, normalized to the main tone's power, are

$$|x_{IM}(t)|^2 = \frac{\Delta G^2 + \Delta\Phi^2}{4} \tag{9a}$$

$$|x_{LO}(t)|^2 = I_{DC}{}^2 + Q_{DC}{}^2 . \tag{9b}$$

Upon measuring the initial power levels, these two equations define circles in the ΔG-$\Delta\Phi$ and I_{DC}-Q_{DC} planes. The DAR system applies small changes to the gain and phase difference between the I and Q channels on the DDS of the transmitter corresponding to points on the circle defined by (9a) while it monitors the subsequent power level of the image frequency tone measured by the receiver element. It starts by picking three points on the circle 120° apart and recording the image tone levels, and from then on it picks a point along the circle in between the two points that have previously given the smallest measured image tone levels. It repeats this until the tone is below a certain threshold (in this case, -60 dBc) or the iteration limit is reached, at which point the procedure is repeated using the point in the plane that has given the best image tone level as the initial measurement point. The procedure is simultaneously and independently performed on the DC offsets in an attempt to find the point in the I_{DC}-Q_{DC} plane that minimizes the measured LO tone level. After both the LO and image tones have been suppressed to 60 dBc, the received spectrum is then dominated by the receiver's LO and image tones caused by the single transmit tone. The DC offsets and quadrature imbalances in the receiver can be directly calculated from the received waveform. The procedure is repeated for other element pairs until each transceiver is fully calibrated.

The DAR system enforces these small digital changes to the waveforms on transmit using the programmability of the DDS at each element, as discussed in Section II. On receive, this is done with the following linear transformation on each element:

$$\begin{bmatrix} I' \\ Q' \end{bmatrix} = \mathbf{A}\left(\begin{bmatrix} I \\ Q \end{bmatrix} - \begin{bmatrix} I_{DC} \\ Q_{DC} \end{bmatrix} \right). \tag{10}$$

Here, I' and Q' are the samples, I and Q are the input samples, I_{DC} and Q_{DC} are simply the DC offsets determined by the above procedure, and the matrix $\mathbf{A}$ is given by:

$$\mathbf{A} = A_E \begin{bmatrix} \cos(\theta_E) & -\sin(\theta_E) \\ \sin(\theta_E) & \cos(\theta_E) \end{bmatrix} \begin{bmatrix} \cos\left(\frac{\Delta\Phi}{2}\right) & \sin\left(\frac{\Delta\Phi}{2}\right) \\ \sin\left(\frac{\Delta\Phi}{2}\right) & \cos\left(\frac{\Delta\Phi}{2}\right) \end{bmatrix} \begin{bmatrix} A_I & 0 \\ 0 & A_Q \end{bmatrix} . \quad (11)$$

Standard phase shifting (θ_E) and element weighting (A_E) are incorporated in the first two terms in (11), and the last two perform the phase and amplitude balancing, respectively.

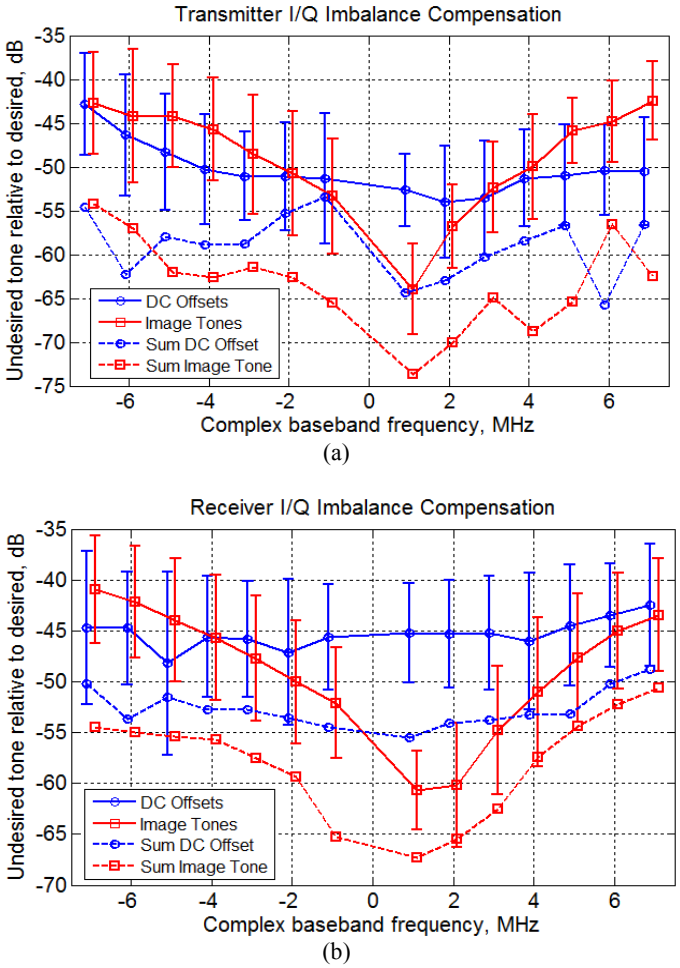

Fig. 9. Quadrature imbalance and DC offset correction performance for a) transmit and b) receive. Solid lines are averages among elements, error bars show standard deviation among elements, and dotted lines are for the overall phase-aligned sum.

The results of this internal calibration performed on the DAR, as validated using external equipment, are shown in Fig. 9. The initial levels of the undesired tones were on the order of 20-30 dB below the main tone for each transceiver, so the compensated results show a marked improvement. The procedure was performed as discussed above at a baseband frequency of 1.1 MHz, chosen to be near the center of the complex baseband but far enough away from DC to isolate the tones. The convergence criteria of -60 dBc on the image tone has been met for nearly all elements. The DC offset (or LO) tone, however, tends to drift with time and temperature, so even if convergence is achieved initially at -60 dBc it will not remain that low very long. The important metric for the system is the image tone of the overall signal, which in this case is represented by the phase-aligned sums. From the results, it is clear that adding additional elements should decrease the relative imbalance tone levels because the phase of each element's imbalance tone is ideally random.

Whether or not the performance achieved by the above calibration procedure has a wide enough bandwidth depends on the application. There are techniques for extending the bandwidth of the quadrature balance with increased digital processing [17]. Regardless, the question of how well the overall system will perform for wideband applications is valid, especially when time-sidelobes and wide-band jammer suppression is of concern. While the subject is mentioned here in the context if quadrature balance, discussions on wideband array performance usually focus on the quality of element-level equalization and the extent to which the beamforming process can accurately steer the beam over a wide range of frequencies, as explained in Rotman and Tur [18]. The work in [19] demonstrates element-level equalization on a digital phased array for both stretch and standard radar processing, though at the time the processing was done off-line. In the DAR system, real-time processing would be implemented with a modified finite impulse response (FIR) filter at the element level in place of the processing done in (10), which is essentially a 1-tap FIR filter. Future revisions of the DAR prototype will explore this possibility. As pointed out in Rotman and Tur, having an independent receiver on each element would enhance the ability to calibrate the system and enable ideal wideband array performance. It is believed that the techniques presented in this and the previous section—which take advantage of the extensive control and digitization of each element on both transmit and receive—could be effectively extended for digital arrays with wider bandwidths; this is a subject for further research.

Conclusion

A phased array radar prototype with digitization at every element has been shown to be capable of maintaining its initial calibration and monitoring its quadrature imbalance after it has been fielded using techniques afforded by its full, digital interface to each transmitter and receiver. These techniques may prove to be very useful in the deployment of future digital phased arrays where precise amplitude and phase control must be maintained for high quality beamforming.

Acknowledgement

This work was sponsored by CERDEC (U.S. Army) with collaboration and contributions from Sierra Monolithics, Inc., Lockheed Martin, and CREE Semiconductor.

REFERENCES

[1] D. Kelley and W. Stutzman, "Array antenna pattern modeling methods that include mutual coupling effects," *IEEE Trans. Ant. Prop.*, vol. 41, no. 12, December 1993.

[2] A. Dreher, N. Niklasch, F. Klefenz, and A. Schroth, "Antenna and receiver system with digital beamforming for satellite navigation and communications," *IEEE Trans. Microwave Theory and Techniques*, vol. 51, no. 7, pp. 1815-1821, July 2003.

[3] L. Kuehnke, "Phased array calibration procedures based on measured element patterns," *Antennas and Propagation, 11th Intl. Conference on*, 17-20 April 2001.

[4] A. Agrawal, and A. Jablon, "A calibration technique for active phased array antennas," *Phased Array Systems and Technology, 2003. IEEE Intl. Symposium on*, pp. 223-228, October 2003

[5] K. Lee, R. Chu, and S. Liu, "A built-in performance-monitoring/fault isolation and correction (PM/FIC) system for active phased-array antennas," *IEEE Trans. Ant. Prop.*, vol. 41, no. 11, November 1993.

[6] H. Aumann, A. Fenn, and F. Willwerth, "Phased array antenna calibration and pattern prediction using mutual coupling measurements," *IEEE Trans. Ant. Prop.*, vol. 37, no. 7, July 1989.

[7] C. Shipley and D. Woods, "Mutual coupling-based calibration of phased array antennas," *Phased Array Systems and Technology, IEEE Intl. Conf. on*, pp. 529-532, 2000.

[8] C. Fulton, P. Clough, V. Pai, and W. Chappell, "A digital array radar with a hierarchical system architecture," *2009 IEEE MTT-S Int. Microwave Symp. Dig.*, pp. 89-92, June 2009.

[9] C. Fulton and W. Chappell, "Low-cost, panelized digital array radar antennas," *COMCAS 2008, IEEE Intl. Conference on*, 13-14 May 2008.

[10] G. Hampson, A. Smolders, "A fast and accurate scheme for calibration of active phased-array antennas," *IEEE Intl. Sym. Ant. Prop. Society*, vol. 2, pp. 1040-1043, August 1999.

[11] S. Mano and T. Katagi, "A method for measuring amplitude and phase of each radiating element of a phased array antenna." *Trans. IECE*, vol. J65-B, no. 5 pp. 555-560. May 1982.

[12] T. Takahashi et al., "Fast measurement technique for phased array calibration," *IEEE Trans. Ant. Prop.*, vol. 56, no. 7, July 2008.

[13] J. Scheer, "Coherent radar system performance estimation," *IEEE Intl. Radar Conf.*, pp. 125-128, May 1990.

[14] A Sinsky and P Wang, "Error analysis of a quadrature coherent detector processor," *IEEE Trans. Aerospace and Electronic Systems*, November 1974.

[15] W. Lilei and X. Huimin, "IQ imbalance compensation in OFDMA based WIMAX digital receivers," *Computer Science and Technology 2008, Intl. Conf. on*, 2008.

[16] M. Windisch, G. Fettweis, "Adaptive I/Q imbalance compensation in low-IF transmitter architectures," *60th IEEE Vehicular Technology Conf.*, vol. 3, pp. 2096-2100, September 2004.

[17] R. Palipana and K. Chung, "FPGA implementation of wideband IQ imbalance correction in OFDM receivers," *4th IEEE Intl. Conf. on Circuits and Systems for Communications*, pp. 663-667, May 2008.

[18] R. Rotman and M. Tur, "Calibration of pulsed phased arrays with wide instantaneous bandwidths," *Ant. Prop., IEEE Intl. Symp. on*, pp. 121-124, June 2007.

[19] D. Rabideau et al., "An S-band digital array radar testbed," *Phased Array Systems and Technology, IEEE Intl. Symp. on*, pp. 113-118, Oct. 2003.